The GPR120 Agonist TUG-891 Alleviates Neuronal Pyroptosis by Inhibiting Endoplasmic Reticulum Stress after Experimental Intraventricular Hemorrhage in Mice

Haoxiang Wang
Sichuan University Engineering Library: Sichuan University
Chang Liu
Sichuan University West China Hospital
Yuanyou Li
Sichuan University West China Hospital
Yi Cao
Chengdu Second People's Hospital
Long Zhao
Affiliated Hospital of North Sichuan Medical College
Yanjie Zhao
Sichuan University West China Hospital
Ziang Deng
Sichuan University West China Hospital
Aiping Tong
Sichuan University State Key Laboratory of Biotherapy
Liangxue Zhou (zhlxlll@163.com)
Sichuan University West China Hospital https://orcid.org/0000-0001-9991-6358

Research Article

Keywords: central nervous system, endoplasmic reticulum stress, pyroptosis, hemorrhagic stroke, neuron, hippocampi, NLRP3, TUG-891, GSDMD, autologous blood injection, neurolog-ical function

Posted Date: April 22nd, 2022

DOI: https://doi.org/10.21203/rs.3.rs-1537154/v1

Abstract

Intraventricular hemorrhage (IVH) is a disease with high disability and mortality rate and lacks specific therapy, and which basic causes lies in the unclear mechanism. Recently, the pyroptosis in central nervous system diseases has received more attention, which is closely related to traumatic brain injury and hemorrhagic stroke. Furthermore, excessive endoplasmic reticulum stress can cause dysfunction of endoplasmic reticulum and even cell pyroptosis by regulating NLRP3 pathway. However, the relationship between pyroptosis and endoplasmic reticulum stress after IVH is unclear. In this study, we investigated the role of endoplasmic reticulum stress and its relationship with pyroptosis in a mouse model of IVH. Our results show that intracerebroventricular injection of autologous blood induced pyroptosis and endoplasmic reticulum stress. The mechanism is that after IVH, the endoplasmic reticulum stress–NLRP3 inflammatory body–pyroptosis pathway is activated, which results in brain tissue damage. This effect can be reversed by the combination of TUG-891 and GPR120. In summary, we revealed that TUG-891 inhibits endoplasmic reticulum stress and reduces neuronal pyroptosis by activating GPR120, which might be a therapeutic target for the treatment of IVH.

Introduction

Intraventricular hemorrhage (IVH), a common clinical critical disease, is divided into primary and secondary intraventricular hemorrhage (Bhattathiri, Gregson et al. 2006, Rosen, Macdonald et al. 2007, Hanley 2009). IVH has the following characteristics: high mortality, high disability rate(Hwang, Bruce et al. 2012), and poor prognosis (Hemphill, Bonovich et al. 2001). However, the causes of the above disastrous prognosis are complex and not fully understood in IVH. Recently, as an important factor of neuropathy, nonapoptotic inflammatory cell death has attracted more and more attention in traumatic brain injury and hemorrhagic stroke (Chang, Lin et al. 2013, Tan, Tan et al. 2014, Sen 2019). Studies have shown that the classical pyroptosis pathway, characterized by nucleotide-binding oligomerization domain, leucine-rich repeat, and pyrin domain–containing protein 3 (NLRP3) inflammasomes, plays an important role in the occurrence, development and prognosis of hemorrhagic stroke(McKenzie, Dixit et al. 2020). In the classic pyroptosis way, activation of NLRP3 inflammasome generate cleaved Caspase-1, which also cleaves gasdermin D(GSDMD) to liberate the N domain of GSDMD(GSDMD-NT) (Ding, Wang et al. 2016, Feng, Fox et al. 2018). The N-terminal of GSDMD locates on the cell membrane and aggregates into pores (Galluzzi, Vitale et al. 2018). In addition, Caspase-1 cleaved pro-IL-1β and pro-IL-18 to form mature IL-1β and IL-18, which is secreted through the membrane pores to the outside of the membrane, and then, inflammation and apoptosis occur (Chen and Nuñez 2010, Franchi, Muñoz-Planillo et al. 2012, Kayagaki, Stowe et al. 2015). Importantly, the inhibition of Caspase-1 by AC-YVAD-CMK (a selective inhibitor of Caspase-1) reduces the brain injury induced by collagenase in ICH mouse model, which proves the importance of pyroptosis in the mechanism of nervous system injury (Lin, Ye et al. 2018, Zhao, Chen et al. 2018).

It has been reported that activation of NLRP3 inflammasome is related to misfolded protein aggregation (Shi, Kouadir et al. 2015). Endoplasmic reticulum is an organelle responsible for protein assembly and

folding in cells (Saibil 2013, Westrate, Lee et al. 2015). Under stress conditions, the endoplasmic reticulum encounters the aggregation of misfolded and unfolded proteins, and then induces unfolded protein response (UPR) and endoplasmic reticulum stress; Sustained or excessive endoplasmic reticulum stress can lead to cell damage and even death (Kim, Xu et al. 2008). Endoplasmic reticulum stress signals are mainly initiated by three effector proteins, the protein kinase RNA-like endoplasmic reticulum kinase (PERK), inositol-requiring protein-1 (IRE1), and activating transcription factor-6 (ATF6) (Bernales, Papa et al. 2006, Marciniak and Ron 2006). These three transmembrane protein sensors are responsible for restoring internal environmental stability during UPR and are kept inactive by binding immunoglobulin (BIP) (Schröder and Kaufman 2005, Ron and Walter 2007). However, during endoplasmic reticulum stress or UPR, BIP separates from effector proteins, resulting in sequential activation of downstream proteins (Mohammed Thangameeran, Tsai et al. 2020). Studies have confirmed that endoplasmic reticulum stress has the potential to induce pyroptosis in some models (Yang, Yao et al. 2014, Lebeaupin, Proics et al. 2015, Chen, Guo et al. 2019). However, there are few studies on endoplasmic reticulum stress and pyroptosis in IVH.

In our study, we focused on the effect of inhibiting endoplasmic reticulum stress on nervous system pyroptosis. TUG-891 is a novel, selectively synthesized GPR120 agonist, which has been used in various studies (Schilperoort, van Dam et al. 2018, Senatorov and Moniri 2018, Wang, He et al. 2019, Huang, Guo et al. 2020). After being activated by ligands, GPR120 plays a role in ameliorating inflammation, enhancing insulin sensitivity and changing lipid metabolism (Moniri 2016). The inhibitory effect of TUG-891 on endoplasmic reticulum stress has also been confirmed in other models (Huang, Guo et al. 2020). Therefore, we hypothesized that TUG-891 can reduce neuronal pyroptosis by inhibiting endoplasmic reticulum stress and play a neuroprotective role, aiming to provide a new strategy of the treatment for IVH patients

Materials And Methods

Experiment animals

108 mice (C57BL/6, weighing 18-24g) were prepared for our experiments. They were bought from the Laboratory Animal Center of Sichuan University. The mice were placed in animal rooms with aseptic, tightly controlled temperature and humidity, 12h light / dark cycle, and could freely obtain food and water. All animal protocols were approved by the Animal Care and Use Committee of Sichuan University.

Mouse model of IVH

Mice were accepted either sham surgery or IVH. The IVH model was built by autologous blood injection. The mice were anesthetized with pentobarbital (40mg/kg intraperitoneally). The skin was cut along the midline of the neck, the muscles were separated, and the skull top was exposed under sterile conditions (use hydrogen peroxide disinfection). Then, the animal was positioned by a stereotaxic frame and a needle (Hamilton, Switzerland) was inserted into the right lateral ventricle (coordinates: 2.5mm ventral, 1.0mm lateral and 0.5mm posterior to the bregma) through a drilled cranial hole(1mm). After that, the

autologous blood was collected from the tail vein of mouse, and it was injected into the right ventricle at a dose of 40ul at a rate of 5ul/min. The needles were left in place for 10min after the injection (Zhu, Gao et al. 2022). In contrast, mice in the sham group only received scalp incision, skull perforation, and needle insertion with no autologous blood injection. Mice were held in the facility at least 3 days before IVH induction.

Drug Administration

TUG-891 was purchased from MCE. TUG-891 was dissolved in 10ml cosolvent composed of 10% DMSO, 40% PEG300, 5% Tween-80 and 45% saline. It was administered in the IVH + TUG-891 group by intraperitoneal injection. The IVH + vehicle group was received an equal dose of the cosolvent.

Experimental design

In this study, all mice were randomly assigned to the following experiments (Fig. 1).

Experiment 1 To assess the expression of NLRP3, GSDMD, IL-1β, ASC and caspase-1 over time in the hippocampus tissue of mice after IVH, we induced the IVH model mice and analyzed by western blots after 18 hours, 36 hours, 54 hours and 72 hours later (n = 6). Based on the outcomes of western blots, we used the most obvious time (72h) of neuronal pyroptosis in IVH model to the remainder of our study. To explore the cellular localization of pyroptosis, immunofluorescence staining was performed after IVH 24 hours and 72 hours (n = 6). GSDMD, IL-1β, NLRP3 and Caspase-1 were co-expressed with neuron-specific nuclear proteins (NeuN). We also performed an immunohistochemical staining and obtain similar results. Mice in control group was received sham surgery.

Experiment2 In order to evaluate whether endoplasmic reticulum stress occurs after IVH and the effect of inhibitory endoplasmic reticulum stress of selective GPR120 agonist TUG-891, mice were randomly divided into 4 groups (n = 6): sham surgery, IVH, IVH + vehicle, IVH + TUG-891. To evaluate the expression of endoplasmic reticulum stress related proteins(CHOP, ATF-4, Bip, IRE1α) in hippocampal tissues, western blot was performed 72 hours after IVH. We stained CHOP and ATF-4 in the periventricular area and hippocampus by immunofluorescence staining. The average number of positive cells (400xmagnification) was counted (n = 3).

Experiment3 To assess the impact of GPR120 inhibition with 35mg/kg (Schilperoort, van Dam et al. 2018) TUG-891 on neuronal pyroptosis, we performed immunofluorescence staining (n = 6) and western blot (n = 6) 72 hours after IVH. We stained GSDMD and NLRP3 in the hippocampus regions by immunofluorescence staining. The average number of positive cells (400xmagnification) was counted (n = 3).

Experiment4 To evaluate the recent neuroprotective impact of TUG-891 on IVH model mice, we observed and evaluated the motor function. We conducted Wire-hanging test to evaluate grip strength and endurance in each mouse on 3 days post-IVH (Zhu, Gao et al. 2014, Zhu, Cao et al. 2017). We also evaluate the neurological function of each mouse, including body symmetry, gait, climbing, circling

behavior, forelimb symmetry, mandatory rotation test and whisker response (Zhu, Gao et al. 2022). The score of each test is 0–4, with a maximum of 28 points.

Western blot analysis

Mice were euthanized after IVH (n = 6), and total proteins were harvested from the hippocampus in radioimmunoprecipitation assay (RIPA) lysis buffer. We transferred the proteins to polyvinylidene fluoride membranes (Millipore), which were blocked with 5% bovine serum albumin (BSA) for 1 hour at room temperature and incubated overnight with following primary antibodies at 4℃:anti-bodies against GSDMDC1(1:100; Santa Cruz, sc-395381), NLRP3(1:200; Santa Cruz, sc-134306), IL-1β(1:1000; Abcam, ab254306), Cleaved Caspase-1(1:1000; Cell Sign Technology, 4199), ASC(1:1000; Cell Sign Technology, 67824), CHOP(1:1000; Cell Sign Technology, 2895), BIP(1:1000; Cell Sign Technology, 3177), ATF-4(1:1000; Cell Sign Technology, 11815) and IRE1α(1:1000; proteintech, 27528). After that, the blots were incubated with horseradish peroxidase (HRP)-conjugated secondary antibody for 1h at room temperature. Finally, the results were quantified by Image J (NIH, USA).

Measurement of Brain Water Content

As previously described (Chen, Gao et al. 2020), we used the wet/dry weight method to measure the brain water content. After complete anesthesia with pentobarbital, the mice brains were quickly removed and divided into cerebrum and cerebellum. Samples were weighed with an electronic analytical balance to calculate the wet weight. To obtain the dry weight of samples, they were dried at 160℃ for 24 hours. We use the following formula to calculate brain water content: [(wet weight-dry weight)/wet weight] × 100%.

Immunohistochemistry and immunofluorescence analysis

Mice were sacrificed at 24h or 72h after IVH induction. We prepared a series of 10 um flakes to perform double immunofluorescence staining and immunohistochemistry. For immunohistochemistry, mouse brain tissue sections were incubated with mouse anti-GSDMDC1 (1:50, Santa Cruz) at 4 ℃ overnight. For immunofluorescence, brain tissue sections were incubated with anti-NeuN antibody, mouse anti-GSDMDC1(1:50, Santa Cruz, sc-395381), mouse anti-NLRP3(1:50, Santa Cruz, sc-134306), mouse anti-CHOP (1:400, Cell Sign Technology, 2895) and rabbit anti-ATF-4(1:200, Cell Sign Technology). After washing with PBS for 3 times, the slices were incubated with corresponding secondary antibodies at room temperature for 2 h. The fluorescence images of hippocampus were obtained under Olympus fluorescence microscope. The positive cells were counted in 4 slides per mouse, and the date were expressed as the ratio of positive cells.

Magnetic resonance imaging (MRI)

Mice were anaesthetized by using a 2% isoflurane-air mixture during MRI. MRI was performed a 7.0-Tesla MR scanner (Bruker BioSpec 70/30 MRI) after injecting autologous blood. We select the following parameters: field of view 35x35mm; matrix 256x256; layer thickness 1mm; echo time 2.5ms and repetition time 100ms.

Neurological Function assessment

As previously described, we used nerve function test and Wire-hanging test, which were blindly evaluated by independent researchers. The Wire-hanging test was used to evaluate the grip strength, balance and endurance of mice. Briefly, the posterior limbs of the mouse were bound with tape, and the forelimbs were hung on a 55cm iron wire 50 cm above the ground. A small pillow was used on the ground to prevent falling. [31] The time each mouse stayed on the wire was recorded.

Nissl Staining

Nissl staining was performed to observe the degeneration of neurons in different areas of the ipsilateral brain (such as hippocampus, perihematomal tissue around lateral ventricle, and normal brain tissue) of mice. We prepared 10um frozen sections, which were dehydrated with 75% and 95% ethanol and washed with distilled water for 5min. Then slices were cultured with Nissl staining solution at room temperature for 20min, and then washed with distilled water for 5min. After dehydration with 75% and 95% ethanol, the slices were added to xylene for 10min. We used a 200x microscope (company) to observe whether there were degenerative neurons in hippocampal CA1 and CA3 regions.

Statistical analysis

Statistical analysis was conducted by using GraphPad Prism (San Diego, USA). Data was expressed as mean ± SD. Statistical differences among different groups were analysed by using Student's t-test. P-value < 0.05 was considered statistically significant.

Results

Weight decreased, ependyma cilia and hippocampus damaged after IVH

The weight of mice in IVH group was lower than that in sham group at different time points (Fig. 2A). Brain tissue sections and 7.0T MRI showed enlargement of the lateral ventricle after IVH (Fig. 2B, C). Nissl staining showed that the number of surviving neurons decreased in IVH group compared with sham group (Fig. 2D). HE staining revealed the ventricle was enlarged, choroid plexus was damaged, ependymal cilia were destroyed in lateral ventricle region, and cell body atrophy, nuclear edge aggregation in hippocampus in IVH group (Fig. 2E). The immunohistochemical results showed that the expression of GSDMD in IVH group was significantly higher than that in sham group, which showed that IVH induced the activation of GSDMD, and promoted the occurrence of pyroptosis (Fig. 2F).

Temporal expression of pyroptosis proteins and spatial expression of GSDMD and NLRP3

The expression of GSDMD, ASC, NLRP3, Caspase-1 and IL-1β at 18h, 36h, 54h and 72h post-IVH in the right hemispheres were evaluated by western blot. The results showed that the expression of all five proteins in IVH group increased compared with sham group, and most proteins reached the peak at 72 hours (Fig. 3, A-F). Double immunofluorescence staining showed that GSDMD and NLRP3 co-localized

with neurons, and the number of GSDMD and NLRP3 positive neurons in hippocampus 72h post-IVH group was significantly higher than that in sham group and 24h post -IVH group (Fig. 3, G-J). Based on our experimental results, 72h post-IVH group was identified as the time node of IVH.

TUG-891 alleviates neuronal endoplasmic reticulum stress after IVH

Western blot was performed among sham, IVH + TUG-891, IVH + DMOS and IVH groups at 72h post-IVH. The results showed that the expression of endoplasmic reticulum stress proteins increased in IVH group, which could be suppressed by TUG-891(Fig. 4, A-E). Double immunofluorescence staining showed that endoplasmic reticulum stress was activated in IVH group, while TUG-891 could inhibit it. (Fig. 4, F-I)

The effects of TUG-891 on neuronal pyroptosis after IVH

Western blot was performed among sham, IVH + TUG-891, IVH + DMOS and IVH groups at 72h post-IVH. The results showed that the expression of pyrolytic proteins was suppressed by TUG-891 (Fig. 5, A-F). Furthermore, double immunofluorescence staining showed that the number of NLRP3 and GSDMD positive neurons decreased, which also confirmed that TUG-891 could inhibit neuronal pyroptosis. (Fig. 5, G-J)

TUG-891 alleviates neuromotor dysfunction after IVH

We measured the weight changes of mice between different groups, we found that TUG-891 could not reverse weight loss in mice after IVH (Fig. 6A). Brain wet and dry weights were measured, and the degree of brain edema was observed (n = 6). Compared with sham group, IVH caused striatal edema. The water content of striatum in IVH + TUG-891 group was significantly lower than that in IVH group (Fig. 6B). We performed neurologic deficits assessment and wire-hanging tests on sham group, IVH + TUG-891 group, IVH + DMSO group and IVH group. The results showed that TUG-891 significantly reversed the neurological deficit of IVH mice and mice in the TUG-891 groups persisted longer on the wire than that in the IVH groups (Fig. 6C, D). Furthermore, there was no significant difference between IVH + DMSO group and IVH group. This is consistent with the aforementioned findings that TUG-891 can inhibit neuronal pyroptosis.

Discussion

In this study, we established IVH model by intracerebroventricular injection of autologous blood, and used TUG-891 to inhibit endoplasmic reticulum stress in order to reduce pyroptosis and protect brain tissue. The experimental results are as follows: (1) IVH activates BIP, ATF-4, CHOP and IRE-1α and induces endoplasmic reticulum stress in mouse neurons. (2) GSDMD and NLRP3 were co-expressed with NeuN neurons after IVH. (3) Endoplasmic reticulum stress inhibitor TUG-891 can reduce neuronal pyroptosis and produce neuroprotective effect. (4) The inhibition of endoplasmic reticulum stress by TUG-891 may depend on the inhibition of BIP abscission. (5) There might be an interaction between endoplasmic reticulum stress and pyroptosis induced by IVH. These results confirm our hypothesis. We found that

TUG-891 can inhibit the up regulation of BIP, ATF-4 and IRE-1 induced by IVH, and then inhibit the activation of GSDMD, NLRP3 and classical pyrolytic pathway proteins. Moreover, the inhibition of pyroptosis by TUG-891 also ameliorate the impaired motor function of IVH mice. Therefore, our results show that TUG-891 can inhibit neuronal pyroptosis by inhibiting ASC / Caspase-1 / NLRP3 / GSDMD pathway.

Pyroptosis, a gasdermin-mediated programmed necrosis, is characterized by impaired plasma membrane integrity and release of intercellular contents (especially inflammatory factors) (Shi, Gao et al. 2017). Recent studies show that GSDMD is the main effector protein of pyroptosis and N-terminal fragment of GSDMD form the pyroptotic pore (He, Wan et al. 2015, Sborgi, Rühl et al. 2016). NLRP3 inflammasome is composed of sensor protein NLRP3, adaptor-protein apoptosis-related spot-like protein ASC, and effector protein pro-caspase-1 (Mangan, Olhava et al. 2018). The activation of NLRP3 inflammasome leads to the activation of GSDMD and the secretion of inflammatory cytokines IL-18 and IL-1 β. Studies have reported that treatment with specific NLRP3 inhibitor CY-09 can reverse the pyroptosis induced by rTREM-1 (Xu, Hong et al. 2021). GPR120, also known as free fatty acid receptor 4, is involved in the metabolism of long-chain free fatty acids. It has been proved to inhibit inflammation and apoptosis in many models (Schilperoort, van Dam et al. 2018, Wang, He et al. 2019, Huang, Guo et al. 2020). To our knowledge, it is the first time to link endoplasmic reticulum stress and pyroptosis in IVH model, and also the first time to evaluate the therapeutic effect of GPR120 in IVH model.

Therefore, in this study, we analyzed the expression of pyroptosis related factors after IVH first. Compared with sham group, the expression of ASC□IL-1β and caspase-1 in mouse neurons was significantly higher after inducing mouse IVH model. Immunofluorescence staining also showed that the number of positive neurons of NLRP3 and GSDMD was significantly higher, which confirmed the occurrence of pyroptosis after IVH. Due to the high expression of NLRP3, we speculated that there may be differential expression of endoplasmic reticulum stress signal pathway closely related to NLRP3. Our subsequent experiments found that endoplasmic reticulum stress-related proteins were abnormally expressed in IVH, indicating that the occurrence of pyroptosis in IVH was caused by endoplasmic reticulum stress. To confirm our hypothesis, we treated mice with TUG-891, an agonist of endoplasmic reticulum stress. The results showed that the combination of TUG-891 and GPR120 started the corresponding signal pathway, which significantly reduced the endoplasmic reticulum stress of mouse neurons. Then the corresponding NLRP3 related protein was down regulated, resulting in the reduction of pyroptosis and the protection of neuron.

Endoplasmic reticulum stress has been verified in a variety of neurological diseases (Binet, Mawambo et al. 2013, Di Prisco, Huang et al. 2014, Zhang, Jansen-West et al. 2014). Inhibiting endoplasmic reticulum stress may be beneficial to these patients. Endoplasmic reticulum stress can be caused by unfolded proteins in endoplasmic reticulum, which results in UPR. UPR consists of three typical pathways. Generally, it has two functions, promoting hemostasis or apoptosis (Huang, Guo et al. 2020). In our study, we found that when GPR120 activated by TUG-891, it can significantly inhibit endoplasmic reticulum stress, which is manifested in the reduction of ATF-4, chop, IRE1 and the inhibition of BIP abscission.

Therefore, we believe that the protective effect of activating GPR120 on the nervous system is through the inhibition of endoplasmic reticulum stress.

Studies have shown that intracerebral hemorrhage (ICH) can induce UPR and interfere with the folding of normal proteins, which induces endoplasmic reticulum stress (Niu, Dai et al. 2017). To alleviate endoplasmic reticulum stress, the effector of endoplasmic reticulum stress proteins can prevent endoplasmic reticulum protein synthesis and increase the transcription of effective protein folding genes (Schönthal 2012). The key role of cell death signaling pathway mediated by endoplasmic reticulum stress in neurodegenerative diseases has become the main research field (Kim, Xu et al. 2008). However, there are few studies on endoplasmic reticulum stress after IVH. We clarified that the impairment of neuromotor function in mice after IVH is related to neuronal pyroptosis caused by endoplasmic reticulum stress activation. The improvement of motor function in mice by inhibiting endoplasmic reticulum stress suggests that it might be an effective target for the treatment of IVH.

Previous studies have shown that TUG-891 can inhibit endoplasmic reticulum stress and reduce acute kidney injury caused by cisplatin (Huang, Guo et al. 2020). It has been proven that TUG-891 can inhibit inflammation and apoptosis in cerebral ischemia injury and other different disease models (Oh, Talukdar et al. 2010, Ren, Chen et al. 2019). Our results show that TUG-891 can inhibit neuronal pyroptosis and play a neuroprotective role in the mouse IVH model, which may be related to the inhibition of endoplasmic reticulum stress by TUG-891. We also found that the CHOP pathway activated by endoplasmic reticulum stress can induce apoptosis and pyroptosis after IVH. Moreover, ASC, which is a pyroptotic marker, can also regulate p53-Bcl2-associated X protein (Bax) related mitochondrial apoptosis pathway by binding Bax mitochondrial apoptosis pathway by interacting with Bax (Ohtsuka, Ryu et al. 2004). Based on the above conclusions, we infer that there might have some crosstalk between apoptosis and pyroptosis, which might be closely related to endoplasmic reticulum stress. Nevertheless, the relationship between them is still unclear, and further research is needed to explore their correlation, which will help to find new targets for IVH drug therapy.

There are some limitations in the study. Firstly, we only focused on the neurological injury and recovery function in the acute stage of IVH, and did not observe the potential changes at the long-term time point after IVH; Secondly, we only showed the results of pharmacological inhibition of pyroptosis, which was not verified in gene knockout mice (such as GSDMD -/- or NLRP3 -/-). More accurate results should be obtained through gene inhibition. In addition, another major limitation of this experiment is that it has not explored the specific mechanism of endoplasmic reticulum stress caused by IVH. These problems will be discussed in future research.

In summary, the study demonstrated that GPR120 agonist TUG-891 reduces the release of inflammatory mediators by reducing endoplasmic reticulum stress and pyroptosis of neurons, which exerts a neuroprotective effect after IVH in mice. (Figure 7)

Conclusion

This study confirmed that IVH model can be successfully established by autologous blood injection; IVH induced neuronal pyroptosis and endoplasmic reticulum stress. The mechanism is that the endoplasmic reticulum stress–NLRP3–pyroptosis signal pathway is activated after IVH, which induces brain injury. This effect can be reversed by the combination of TUG-891 and GPR120. Therefore, GPR120 might be a therapeutic target for the treatment of IVH.

Declarations

Ethics approval

This study was performed in line with the principles of the Declaration of Helsinki. Approval was granted by the Ethics Committee of Sichuan University.

Data Availability

The datasets generated during and/or analysed during the current study are not publicly available but are available from the corresponding author on reasonable request

Conflict of interest

The authors have no relevant financial or non-financial interests to disclose.

Funding

The authors declare that no funds, grants, or other support were received during the preparation of this manuscript.

Author Contributions

All authors contributed to the study conception and design. Material preparation, data collection and analysis were performed by Haoxiang Wang, Yuanyou Li, Long Zhao, Ziang Deng, and Yanjie Zhao. The first draft of the manuscript was written by Haoxiang Wang, Chang Liu and Yi Cao and all authors commented on previous versions of the manuscript. All authors read and approved the final manuscript.

Acknowledgements

Special thanks go to State Key Laboratory of Biotherapy, West China Medical School, Sichuan University for their experimental site and equipment.

Disclosure of potential conflicts of interest

Not applicable

Research involving Human Participants and/or Animals

Not applicable

Informed consent

Not applicable

References

1. Bernales S, Papa FR, Walter P (2006) Intracellular signaling by the unfolded protein response. Annu Rev Cell Dev Biol 22:487–508
2. Bhattathiri PS, Gregson B, Prasad KS, Mendelow AD (2006) "Intraventricular hemorrhage and hydrocephalus after spontaneous intracerebral hemorrhage: results from the STICH trial". Acta Neurochir Suppl 96:65–68
3. Binet F, Mawambo G, Sitaras N, Tetreault N, Lapalme E, Favret S, Cerani A, Leboeuf D, Tremblay S, Rezende F, Juan AM, Stahl A, Joyal JS, Milot E, Kaufman RJ, Guimond M, Kennedy TE, Sapieha P (2013) "Neuronal ER stress impedes myeloid-cell-induced vascular regeneration through IRE1α degradation of netrin-1". Cell Metab 17(3):353–371
4. Chang W, Lin J, Dong J, Li D (2013) "Pyroptosis: an inflammatory cell death implicates in atherosclerosis. " Med Hypotheses 81(3):484–486
5. Chen G, Gao C, Yan Y, Wang T, Luo C, Zhang M, Chen X, Tao L (2020) "Inhibiting ER Stress Weakens Neuronal Pyroptosis in a Mouse Acute Hemorrhagic Stroke Model. " Mol Neurobiol 57(12):5324–5335
6. Chen GY, Nuñez G (2010) "Sterile inflammation: sensing and reacting to damage". Nat Rev Immunol 10(12):826–837
7. Chen X, Guo X, Ge Q, Zhao Y, Mu H, Zhang J (2019) "ER Stress Activates the NLRP3 Inflammasome: A Novel Mechanism of Atherosclerosis." Oxid Med Cell Longev **2019**: 3462530
8. Di Prisco GV, Huang W, Buffington SA, Hsu CC, Bonnen PE, Placzek AN, Sidrauski C, Krnjević K, Kaufman RJ, Walter P, Costa-Mattioli M (2014) "Translational control of mGluR-dependent long-term depression and object-place learning by eIF2α". Nat Neurosci 17(8):1073–1082
9. Ding J, Wang K, Liu W, She Y, Sun Q, Shi J, Sun H, Wang DC, Shao F (2016) Pore-forming activity and structural autoinhibition of the gasdermin family. Nature 535(7610):111–116
10. Feng S, Fox D, Man SM (2018) "Mechanisms of Gasdermin Family Members in Inflammasome Signaling and Cell Death". J Mol Biol 430(18 Pt B):3068–3080
11. Franchi L, Muñoz-Planillo R, Núñez G (2012) "Sensing and reacting to microbes through the inflammasomes". Nat Immunol 13(4):325–332
12. Galluzzi, L., I. Vitale, S. A. Aaronson, J. M. Abrams, D. Adam, P. Agostinis, E. S.Alnemri, L. Altucci, I. Amelio, D. W. Andrews, M. Annicchiarico-Petruzzelli, A. V.Antonov, E. Arama, E. H. Baehrecke, N. A. Barlev, N. G. Bazan, F. Bernassola, M. J.M. Bertrand, K. Bianchi, M. V. Blagosklonny, K. Blomgren, C. Borner, P. Boya, C. Brenner,M. Campanella, E. Candi, D. Carmona-Gutierrez, F. Cecconi, F. K. Chan, N. S.

Chandel,E. H. Cheng, J. E. Chipuk, J. A. Cidlowski, A. Ciechanover, G. M. Cohen, M. Conrad,J. R. Cubillos-Ruiz, P. E. Czabotar, V. D'Angiolella, T. M. Dawson, V. L. Dawson,V. De Laurenzi, R. De Maria, K. M. Debatin, R. J. DeBerardinis, M. Deshmukh, N. Di Daniele, F. Di Virgilio, V. M. Dixit, S. J. Dixon, C. S. Duckett, B. D. Dynlacht,W. S. El-Deiry, J. W. Elrod, G. M. Fimia, S. Fulda, A. J. García-Sáez, A. D. Garg,C. Garrido, E. Gavathiotis, P. Golstein, E. Gottlieb, D. R. Green, L. A. Greene, H.Gronemeyer, A. Gross, G. Hajnoczky, J. M. Hardwick, I. S. Harris, M. O. Hengartner,C. Hetz, H. Ichijo, M. Jäättelä, B. Joseph, P. J. Jost, P. P. Juin, W. J. Kaiser,M. Karin, T. Kaufmann, O. Kepp, A. Kimchi, R. N. Kitsis, D. J. Klionsky, R. A. Knight,S. Kumar, S. W. Lee, J. J. Lemasters, B. Levine, A. Linkermann, S. A. Lipton, R. A.Lockshin, C. López-Otín, S. W. Lowe, T. Luedde, E. Lugli, M. MacFarlane, F. Madeo,M. Malewicz, W. Malorni, G. Manic, J. C. Marine, S. J. Martin, J. C. Martinou, J.P. Medema, P. Mehlen, P. Meier, S. Melino, E. A. Miao, J. D. Molkentin, U. M. Moll,C. Muñoz-Pinedo, S. Nagata, G. Nuñez, A. Oberst, M. Oren, M. Overholtzer, M. Pagano,T. Panaretakis, M. Pasparakis, J. M. Penninger, D. M. Pereira, S. Pervaiz, M. E. Peter,M. Piacentini, P. Pinton, J. H. M. Prehn, H. Puthalakath, G. A. Rabinovich, M. Rehm,R. Rizzuto, C. M. P. Rodrigues, D. C. Rubinsztein, T. Rudel, K. M. Ryan, E. Sayan,L. Scorrano, F. Shao, Y. Shi, J. Silke, H. U. Simon, A. Sistigu, B. R. Stockwell,A. Strasser, G. Szabadkai, S. W. G. Tait, D. Tang, N. Tavernarakis, A. Thorburn, Y.Tsujimoto, B. Turk, T. Vanden Berghe, P. Vandenabeele, M. G. Vander Heiden, A. Villunger,H. W. Virgin, K. H. Vousden, D. Vucic, E. F. Wagner, H. Walczak, D. Wallach, Y. Wang,J. A. Wells, W. Wood, J. Yuan, Z. Zakeri, B. Zhivotovsky, L. Zitvogel, G. Melino and G. Kroemer (2018). "Molecular mechanisms of cell death: recommendations of the Nomenclature Committee on Cell Death 2018." Cell Death Differ **25**(3): 486–541

13. Hanley DF (2009) Intraventricular hemorrhage: severity factor and treatment target in spontaneous intracerebral hemorrhage. Stroke 40(4):1533–1538
14. He WT, Wan H, Hu L, Chen P, Wang X, Huang Z, Yang ZH, Zhong CQ, Han J (2015) "Gasdermin D is an executor of pyroptosis and required for interleukin-1β secretion. " Cell Res 25(12):1285–1298
15. Hemphill JC 3, Bonovich DC, Besmertis L, Manley GT, Johnston SC (2001) The ICH score: a simple, reliable grading scale for intracerebral hemorrhage. Stroke 32(4):891–897
16. Huang Z, Guo F, Xia Z, Liang Y, Lei S, Tan Z, Ma L, Fu P (2020) "Activation of GPR120 by TUG891 ameliorated cisplatin-induced acute kidney injury via repressing ER stress and apoptosis". Biomed Pharmacother 126:110056
17. Hwang BY, Bruce SS, Appelboom G, Piazza MA, Carpenter AM, Gigante PR, Kellner CP, Ducruet AF, Kellner MA, Deb-Sen R, Vaughan KA, Meyers PM, Connolly ES (2012) Jr. "Evaluation of intraventricular hemorrhage assessment methods for predicting outcome following intracerebral hemorrhage." J Neurosurg **116**(1): 185–192
18. Kayagaki N, Stowe IB, Lee BL, O'Rourke K, Anderson K, Warming S, Cuellar T, Haley B, Roose-Girma M, Phung QT, Liu PS, Lill JR, Li H, Wu J, Kummerfeld S, Zhang J, Lee WP, Snipas SJ, Salvesen GS, Morris LX, Fitzgerald L, Zhang Y, Bertram EM, Goodnow CC, Dixit VM (2015) Caspase-11 cleaves gasdermin D for non-canonical inflammasome signalling. Nature 526(7575):666–671
19. Kim I, Xu W, Reed JC (2008) Cell death and endoplasmic reticulum stress: disease relevance and therapeutic opportunities. Nat Rev Drug Discov 7(12):1013–1030

20. Lebeaupin C, Proics E, de Bieville CH, Rousseau D, Bonnafous S, Patouraux S, Adam G, Lavallard VJ, Rovere C, Le Thuc O, Saint-Paul MC, Anty R, Schneck AS, Iannelli A, Gugenheim J, Tran A, Gual P, Bailly-Maitre B (2015) ER stress induces NLRP3 inflammasome activation and hepatocyte death. Cell Death Dis 6(9):e1879
21. Lin X, Ye H, Siaw-Debrah F, Pan S, He Z, Ni H, Xu Z, Jin K, Zhuge Q, Huang L (2018) "AC-YVAD-CMK Inhibits Pyroptosis and Improves Functional Outcome after Intracerebral Hemorrhage". Biomed Res Int 2018:3706047
22. Mangan MSJ, Olhava EJ, Roush WR, Seidel HM, Glick GD, Latz E (2018) "Targeting the NLRP3 inflammasome in inflammatory diseases". Nat Rev Drug Discov 17(8):588–606
23. Marciniak SJ, Ron D (2006) Endoplasmic reticulum stress signaling in disease. Physiol Rev 86(4):1133–1149
24. McKenzie BA, Dixit VM, Power C (2020) "Fiery Cell Death: Pyroptosis in the Central Nervous System. " Trends Neurosci 43(1):55–73
25. Mohammed Thangameeran SI, Tsai ST, Hung HY, Hu WF, Pang CY, Chen SY, Liew HK (2020) "A Role for Endoplasmic Reticulum Stress inIntracerebral Hemorrhage." Cells**9**(3)
26. Moniri NH (2016) "Free-fatty acid receptor-4 (GPR120): Cellular and molecular function and its role in metabolic disorders". Biochem Pharmacol 110–111:1–15
27. Niu M, Dai X, Zou W, Yu X, Teng W, Chen Q, Sun X, Yu W, Ma H, Liu P (2017) "Autophagy, Endoplasmic Reticulum Stress and the Unfolded Protein Response in Intracerebral Hemorrhage. " Transl Neurosci 8:37–48
28. Oh DY, Talukdar S, Bae EJ, Imamura T, Morinaga H, Fan W, Li P, Lu WJ, Watkins SM, Olefsky JM (2010) GPR120 is an omega-3 fatty acid receptor mediating potent anti-inflammatory and insulin-sensitizing effects. Cell 142(5):687–698
29. Ohtsuka T, Ryu H, Minamishima YA, Macip S, Sagara J, Nakayama KI, Aaronson SA, Lee SW (2004) "ASC is a Bax adaptor and regulates the p53-Bax mitochondrial apoptosis pathway". Nat Cell Biol 6(2):121–128
30. Ren Z, Chen L, Wang Y, Wei X, Zeng S, Zheng Y, Gao C, Liu H (2019) "Activation of the Omega-3 Fatty Acid Receptor GPR120 Protects against Focal Cerebral Ischemic Injury by Preventing Inflammation and Apoptosis in Mice". J Immunol 202(3):747–759
31. Ron D, Walter P (2007) Signal integration in the endoplasmic reticulum unfolded protein response. Nat Rev Mol Cell Biol 8(7):519–529
32. Rosen DS, Macdonald RL, Huo D, Goldenberg FD, Novakovic RL, Frank JI, Rosengart AJ (2007) "Intraventricular hemorrhage from ruptured aneurysm: clinical characteristics, complications, and outcomes in a large, prospective, multicenter study population". J Neurosurg 107(2):261–265
33. Saibil H (2013) "Chaperone machines for protein folding, unfolding and disaggregation". Nat Rev Mol Cell Biol 14(10):630–642
34. Sborgi L, Rühl S, Mulvihill E, Pipercevic J, Heilig R, Stahlberg H, Farady CJ, Müller DJ, Broz P, Hiller S (2016) "GSDMD membrane pore formation constitutes the mechanism of pyroptotic cell death".

Embo j 35(16):1766–1778

35. Schilperoort M, van Dam AD, Hoeke G, Shabalina IG, Okolo A, Hanyaloglu AC, Dib LH, Mol IM, Caengprasath N, Chan YW, Damak S, Miller AR, Coskun T, Shimpukade B, Ulven T, Kooijman S, Rensen PC, Christian M (2018) "The GPR120 agonist TUG-891 promotes metabolic health by stimulating mitochondrial respiration in brown fat."EMBO Mol Med**10**(3)
36. Schönthal AH (2012) "Endoplasmic reticulum stress: its role in disease and novel prospects for therapy." Scientifica (Cairo) **2012**: 857516
37. Schröder M, Kaufman RJ (2005) "ER stress and the unfolded protein response". Mutat Res 569(1–2):29–63
38. Sen N (2019) "ER Stress, CREB, and Memory: A Tangled Emerging Link in Disease. " Neuroscientist 25(5):420–433
39. Senatorov IS, Moniri NH (2018) The role of free-fatty acid receptor-4 (FFA4) in human cancers and cancer cell lines. Biochem Pharmacol 150:170–180
40. Shi F, Kouadir M, Yang Y (2015) "NALP3 inflammasome activation in protein misfolding diseases. " Life Sci 135:9–14
41. Shi J, Gao W, Shao F (2017) "Pyroptosis: Gasdermin-Mediated Programmed Necrotic Cell Death". Trends Biochem Sci 42(4):245–254
42. Tan MS, Tan L, Jiang T, Zhu XC, Wang HF, Jia CD, Yu JT (2014) Amyloid-β induces NLRP1-dependent neuronal pyroptosis in models of Alzheimer's disease. Cell Death Dis 5(8):e1382
43. Wang X, He S, Gu Y, Wang Q, Chu X, Jin M, Xu L, Wu Q, Zhou Q, Wang B, Zhang Y, Wang H, Zheng L (2019) "Fatty acid receptor GPR120 promotes breast cancer chemoresistance by upregulating ABC transporters expression and fatty acid synthesis." EBioMedicine. 40:251–262
44. Westrate LM, Lee JE, Prinz WA, Voeltz GK (2015) "Form follows function: the importance of endoplasmic reticulum shape". Annu Rev Biochem 84:791–811
45. Xu P, Hong Y, Xie Y, Yuan K, Li J, Sun R, Zhang X, Shi X, Li R, Wu J, Liu X, Hu W, Sun W (2021) "TREM-1 Exacerbates Neuroinflammatory Injury via NLRP3 Inflammasome-Mediated Pyroptosis in Experimental Subarachnoid Hemorrhage". Transl Stroke Res 12(4):643–659
46. Yang JR, Yao FH, Zhang JG, Ji ZY, Li KL, Zhan J, Tong YN, Lin LR, He YN (2014) Ischemia-reperfusion induces renal tubule pyroptosis via the CHOP-caspase-11 pathway. Am J Physiol Renal Physiol 306(1):F75–84
47. Zhang YJ, Jansen-West K, Xu YF, Gendron TF, Bieniek KF, Lin WL, Sasaguri H, Caulfield T, Hubbard J, Daughrity L, Chew J, Belzil VV, Prudencio M, Stankowski JN, Castanedes-Casey M, Whitelaw E, Ash PE, DeTure M, Rademakers R, Boylan KB, Dickson DW, Petrucelli L (2014) "Aggregation-prone c9FTD/ALS poly(GA) RAN-translated proteins cause neurotoxicity by inducing ER stress". Acta Neuropathol 128(4):505–524
48. Zhao H, Chen Y, Feng H (2018) "P2X7 Receptor-Associated Programmed Cell Death in the Pathophysiology of Hemorrhagic Stroke. " Curr Neuropharmacol 16(9):1282–1295

49. Zhu W, Cao FS, Feng J, Chen HW, Wan JR, Lu Q, Wang J (2017) NLRP3 inflammasome activation contributes to long-term behavioral alterations in mice injected with lipopolysaccharide. Neuroscience 343:77–84
50. Zhu W, Gao Y, Chang CF, Wan JR, Zhu SS, Wang J (2014) "Mouse models of intracerebral hemorrhage in ventricle, cortex, and hippocampus by injections of autologous blood or collagenase". PLoS ONE 9(5):e97423
51. Zhu W, Gao Y, Wan J, Lan X, Han X, Zhu S, Zang W, Chen X, Ziai W, Hanley DF, Russo SJ, Jorge RE, Wang J (2022) "Corrigendum to "Changes in motor function, cognition, and emotion-related behavior after right hemispheric intracerebral hemorrhage in various brain regions of mouse" [Brain Behav. Immun. 69 (2018) 568–581]." Brain Behav Immun **99**: 409–411

Figures

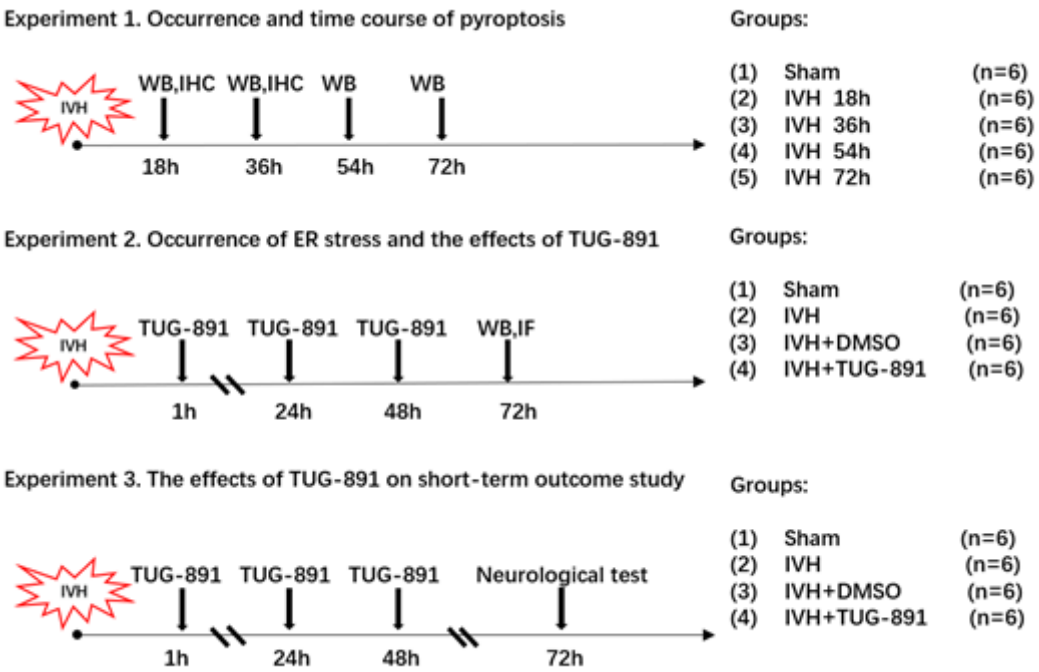

Figure 1

Experimental design and animal groups. WB: western blot; IHC: immunohistochemistry; IF: immunofluorescence

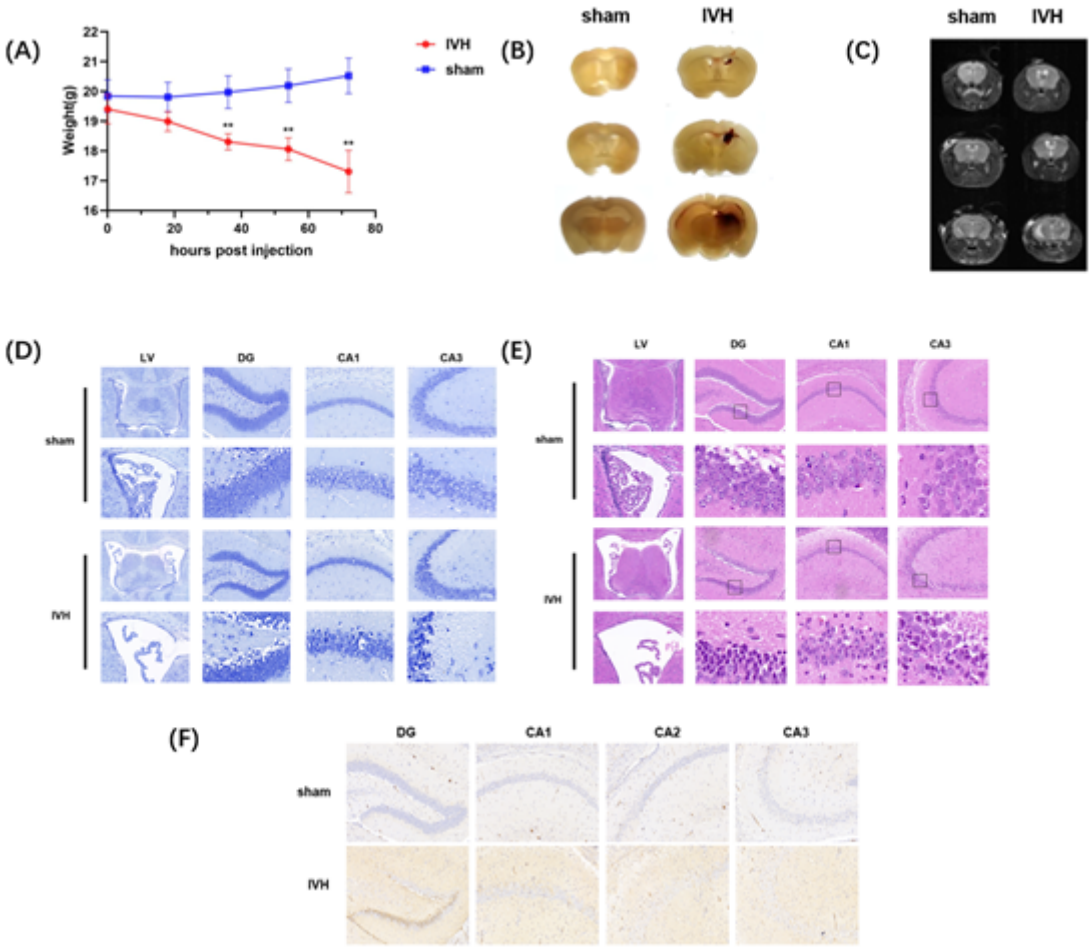

Figure 2

General observation between sham group and IVH group. (A) Changes of body weight with time in IVH group and sham group. (B) Typical appearance of IVH group in coronal incision of mouse brain compared with sham group. (C) MRI showed typical image of IVH in coronal plane of mouse brain compared with sham group. Typical Nissl-stained (D) and HE-stained (E) images of the hippocampal DG, CA1 and CA3 regions from IVH group and sham group. Bar = 200um (LV) or 100um (DG, CA1, CA2, CA3) (F) Representative images of immunohistochemistry staining of GSDMD in hippocampal DG, CA1, CA2 and CA3 regions. Bar = 100um. Data shown are individual values with mean ± SD, n = 6, statistical differences between groups were analyzed by Student's t-test. **p < 0.01 vs. sham

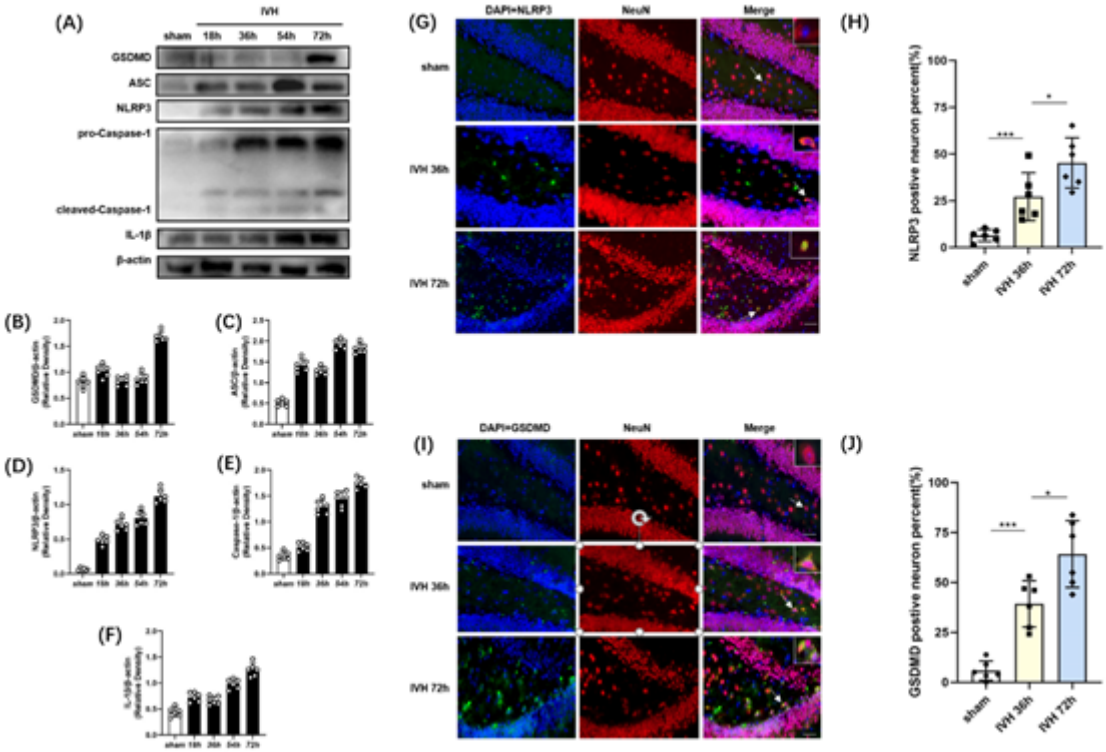

Figure 3

Expression of pyrolytic proteins after IVH. (A) Typical western blot bands of the time-dependent expression of pyrolytic proteins from the ipsilateral hemisphere after IVH. (B-F) Statistical analysis of pyrolytic proteins in different time groups. n=6. (G) Representative immunofluorescence staining images of NeuN (red) and NLRP3 (green) in hippocampal DG region. Nuclei were stained with DAPI (blue). Bar = 30 um. (H) Statistical analysis of NLRP3 positive neurons in different groups. (I) Representative immunofluorescence staining images of NeuN (red) and GSDMD (green) in hippocampal DG region. Nuclei were stained with DAPI (blue). Bar = 30 um. (J) Statistical analysis of GSDMD positive neurons in different groups. Data shown are individual values with mean ± SD, n = 6, statistical differences between groups were analyzed by Student's t-test. *p < 0.05, ***p<0.001.

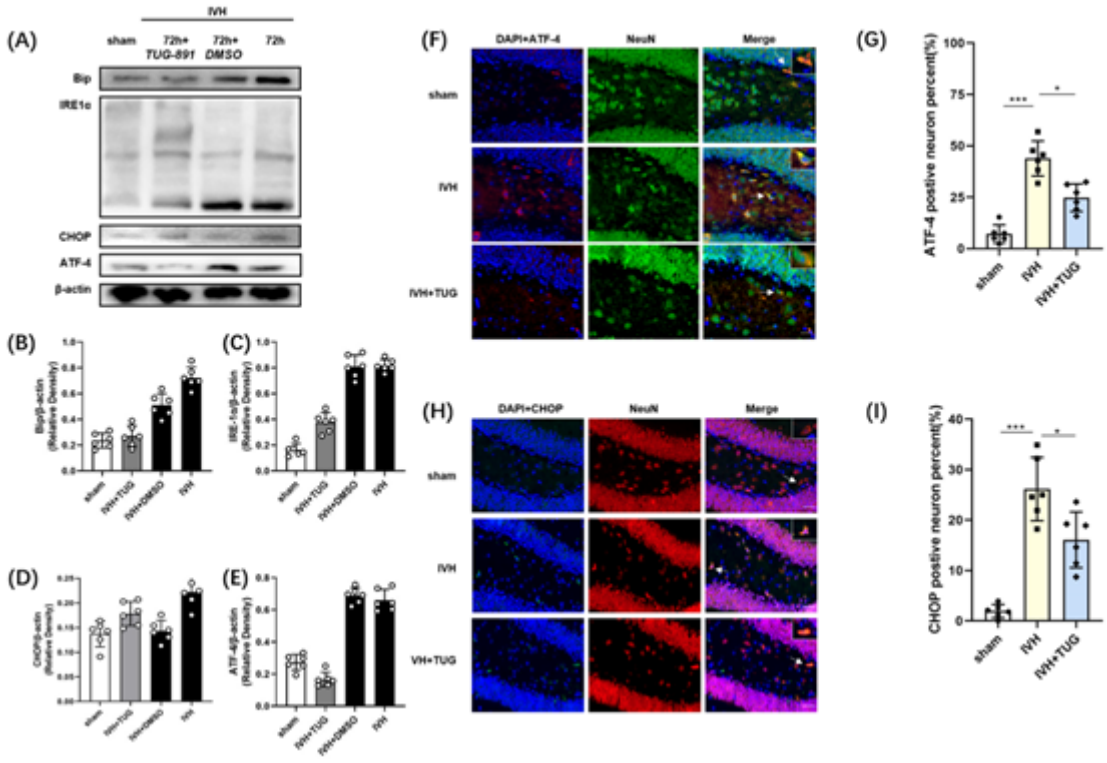

Figure 4

Expression of endoplasmic reticulum stress proteins after IVH and the effects of TUG-891 (TUG) after IVH. (A) Typical western blot bands of the endoplasmic reticulum stress proteins from the ipsilateral hemisphere after IVH. (B-E) Statistical analysis of pyrolytic proteins in different groups. n=6. (F) Representative immunofluorescence staining images of NeuN (green) and ATF-4 (red) in hippocampal DG region. Nuclei were stained with DAPI (blue). Bar = 30 um. (G) Statistical analysis of ATF-4 positive neurons in different groups. (H) Representative immunofluorescence staining images of NeuN (red) and CHOP (green) in hippocampal DG region. Nuclei were stained with DAPI (blue). Bar = 30 um. (I) Statistical analysis of CHOP positive neurons in different groups. Data shown are individual values with mean ± SD, n = 6, statistical differences between groups were analyzed by Student's t-test. *p < 0.05, ***p<0.001.

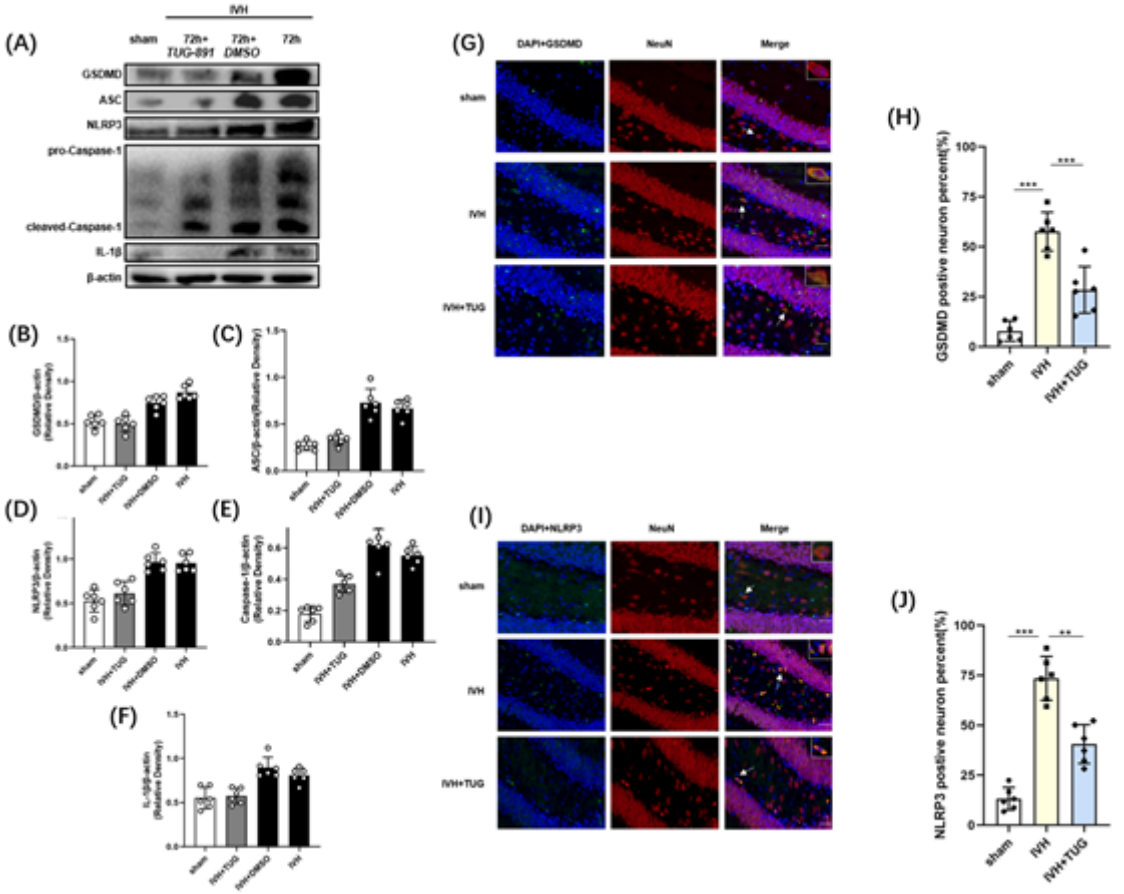

Figure 5

The inhibitory effects of TUG-891 on pyroptosis. (A) Typical western blot bands of the pyrolytic proteins from the ipsilateral hemisphere after IVH. (B-F) Statistical analysis of pyrolytic proteins in different groups. n=6. (G) Representative immunofluorescence staining images of NeuN (red) and GSDMD (green) in hippocampal DG region. Nuclei were stained with DAPI (blue). Bar = 30 um. (H) Statistical analysis of GSDMD positive neurons in different groups. (I) Representative immunofluorescence staining images of NeuN (red) and NLRP3 (green) in hippocampal DG region. Nuclei were stained with DAPI (blue). Bar = 30 um. (J) Statistical analysis of GSDMD positive neurons in different groups. Data shown are individual values with mean ± SD, n = 6, statistical differences between groups were analyzed by Student's t-test. **p < 0.01, ***p<0.001.

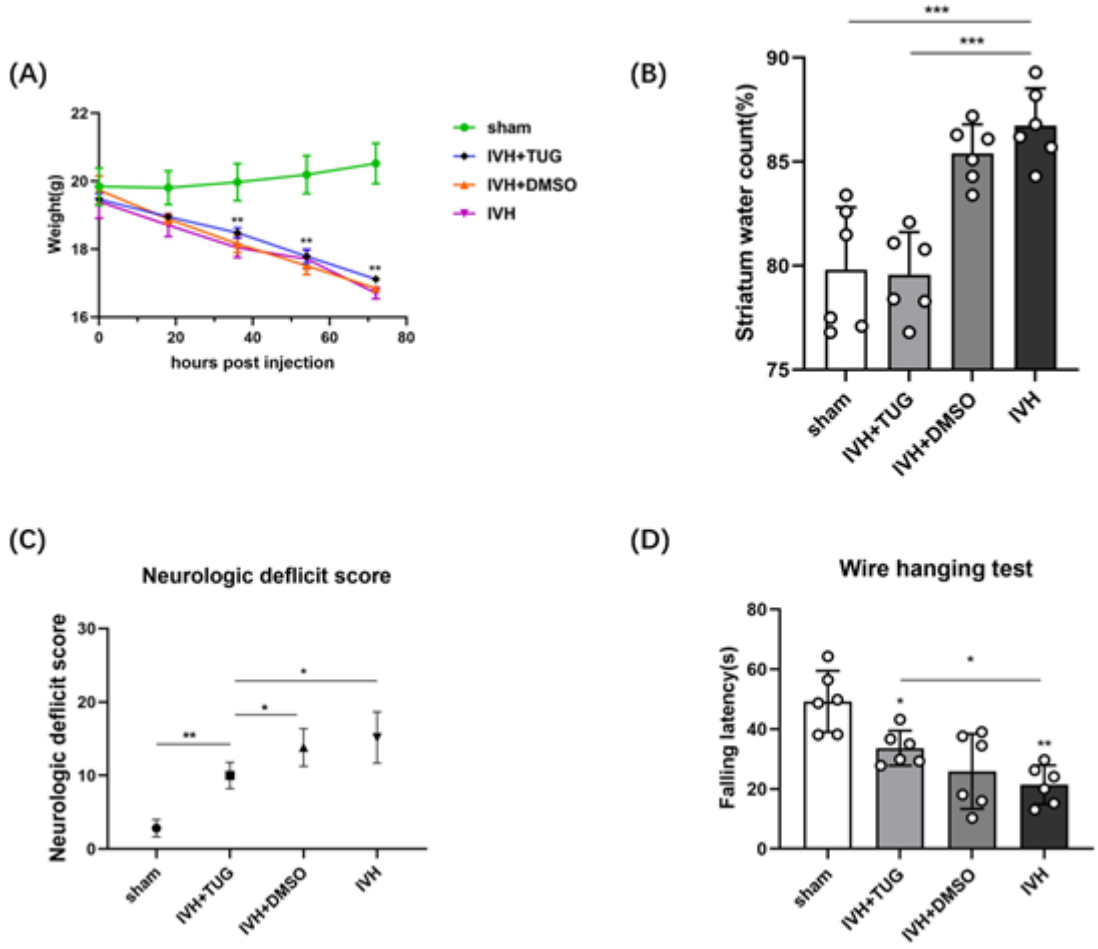

Figure 6

The effects of TUG-891 on body weight, striatum water count and Neurobehavioral outcomes after ICH. (A) Changes of body weight in each group at 18h, 36h, 54h and 72h. (B) TUG-891 treatment reduced striatum water content in comparison with the IVH group (n = 6). (C) Results of neurological function score in different groups. (D) Results of wire hanging test in different groups. Data shown are individual values with mean ± SD, n = 6, statistical differences between groups were analyzed by Student's t-test. **p < 0.01 vs. sham, *p<0.05, ***p<0.01.

Figure 7

The main signal pathway of the study. We injected autologous blood in the ventricle to induce endoplasmic reticulum stress and neuronal pyroptosis in the hippocampus. When we treated mice with TUG-891, the ATF-4-CHOP and IRE-1α pathways of endoplasmic reticulum stress were inhibited. TUG-891 could also reduce neuronal pyroptosis induced by IVH.